2P1-3

Proceedings of Symposium on Ultrasonic Electronics, Vol. 33 (2012) pp. 153-154
13-15 November, 2012

Fiber-Optic Ultrasonic Hydrophone Using Short Fabry-Perot Cavity with Multilayer Reflectors

Kyung-Su Kim[1†], Yosuke Mizuno[1], and Kentaro Nakamura[1] ([1]P&I Lab., Tokyo Tech)
金 景洙 [1†]，水野 洋輔 [1]，中村 健太郎 [1] ([1] 東工大　精密工学研究所)

1. Introduction

Detection of mega-hertz ultrasonic-wave in liquids is of great significance because of its broad application capabilities in both biomedical and industrial fields. Although piezoelectric hydrophones based on polyvinylidene difluoride (PVDF) have been commonly used, small-sized PDVF hydrophones are fragile and sometimes broken by high sound pressure. Besides, the length of their output cable is limited because of the high electric impedance. As alternative sensors, fiber-optic ultrasonic sensors have been developed with such advantages as high spatial resolution, durability against high sound pressure, and immunity to electromagnetic interference. Their typical examples include ultrasonic sensors based on (1) reflection at the fiber end, (2) fiber Bragg gratings (FBGs), (3) fiber Fabry-Perot resonator (FFP) and (4) FFP with distributed Bragg reflectors (DBR) [1-4].

In this study, a BOF sensor is investigated as an ultrasonic probe. 'BOF' means a 'band-pass filter on a fiber end,' and has a similar structure to the FFP with DBRs, but BOF is made through a more sophisticated way and suitable for mass production with lower cost. We present a trial to apply the BOF sensor for mega-hertz ultrasonic wave detection in water. We experimentally show that ultrasonic waves at 1.56 MHz are successfully detected in water with a good signal-to-noise ratio (SNR). We also study the working principle and the characteristics by comparing the ultrasonic sensitivity with that of a conventional hydrophone.

2. BOF structure and operating principle

The BOF is composed of dielectric multilayer films (DMFs) deposited on the crystallized glass, which is connected to the optical fiber end [5]. The DMFs comprising SiO_2 and TiO_2 layers accumulated by ion-assisted evaporation form an optical cavity, which serves as an optical filter. The incident light component with a particular wavelength is selectively eliminated. Two mechanical advantages of the BOF are: (1) the ease of manufacturing DMFs compared with other multilayer hydrophones, and (2) the robustness of the sensor head owing to the lattice match of each layer which enables high-frequency ultrasonic wave detection without damage. **Figure 1(a)** represents the detailed structure of the DMFs, which is a Fabry-Perot composed of a cavity of 925-nm-thick SiO_2 layer and distributed Bragg reflectors (DBRs) on both sides. Each DBR is composed of eight pairs of 215-nm-thick SiO_2 (n=1.46) and 215-nm-thick TiO_2 (n=2.22) layers. The TiO_2 top layer protecting the whole structure is 450-nm thick. The typical reflection characteristics of BOF are illustrated in **Fig. 1(b)**. The sharp refection band is observed around the middle. If the stress is applied to the BOF, the center wavelength λc of the rejection band is shifted in proportion to the magnitude of the stress. On the other hand, we have found that the center wavelength is also sensitive to the refractive index of the media facing at the top layer of BOF [6]. Ultrasonic filed induces both stress to the BOF and refractive index modulation of media (water) surrounding the BOF. Our following experiments will reveal which contribution is major one.

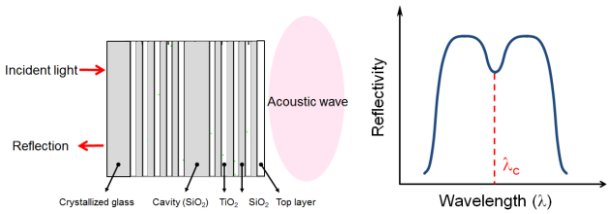

(a) (b)

Fig. 1 (a) Detailed structure of the DMFs. (b) Typical wavelength response of the BOF.

3. Experimental setup and results

Figure 2 shows the experimental setup for ultrasonic wave detection using the BOF-based ultrasonic hydrophone. A tunable laser diode (TLD) of 1550-nm band was used as light source and its output power was fixed at 5 dBm. The output light was injected into the BOF via an optical circulator. The reflected light from the BOF was converted to an electrical signal using a photodiode (PD) with a bandwidth of over 5 MHz, and was monitored employing an oscilloscope (OSC) with a sampling rate of 250 MS/s. By applying burst waves to a disk-shaped PZT transducer (PZT), ultrasonic burst waves at 1.56 MHz were generated. The end of the BOF-based ultrasonic hydrophone was fixed above the center of the PZT transducer. **Figure 3(a)** shows the alternating current (AC) component of the

†kskim@sonic.pi.titech.ac.jp

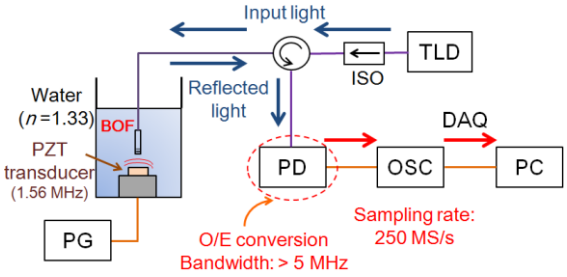

Fig. 2. Schematic experimental setup for ultrasonic-wave measurement. DAQ, data acquisition; ISO, isolator; OSC, oscilloscope; PC, personal computer; PD, photodiode; PG, pulse generator; PZT, lead zirconate titanate; TLD, tunable laser diode.

signal voltage, U_{ac}, measured at the photodiode, when the optical wavelength was 1532.50 nm and the distance between the BOF end and the PZT was 100 mm. The waveform was averaged for 64 shots. For comparison, we also detected the same ultrasonic wave with a conventional needle hydrophone as shown in **Fig. 3(b)**. The obtained waveforms were similar in shape and SNR, which indicates that the BOF-based sensor properly works as an ultrasonic hydrophone. **Figure 4(a)** represents the optical wavelength dependence of the direct current (DC) component of the signal voltage U_{dc} and that of the peak-to-peak value of U_{ac} ($\equiv U_{p\text{-}p}$). The DC component indicates the reflectance of the BOF, while $U_{p\text{-}p}$ shows the amplitude of ultrasonic signal. As can be seen, if we differentiate the curve of the obtained U_{dc} with respect to optical wavelength, the shape of $U_{p\text{-}p}$ can be obtained. The absolute value $U_{p\text{-}p}$ became maximum at 1533.50 and 1535.75 nm; U_{ac} at 1533.50 nm is plotted as negative value, and at 1535.73 nm as positive one,

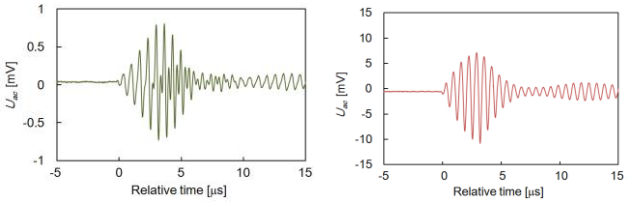

(a) (b)

Fig. 3. (a) U_{ac} measured with (a) the BOF-based ultrasonic hydrophone, and (b) the conventional needle hydrophone.

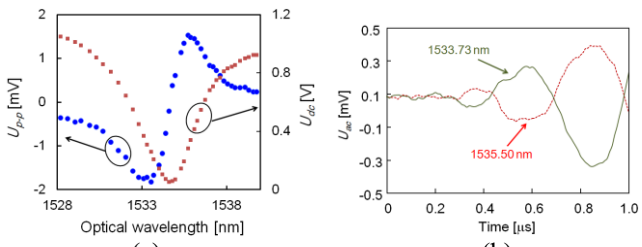

(a) (b)

Fig. 4. (a) $U_{p\text{-}p}$ and U_{dc} as functions of optical wavelength. (b) Waveforms of U_{ac} at 1533.50 and 1535.73nm.

†kskim@sonic.pi.titech.ac.jp

because the U_{ac} waveforms at 1533.73 nm and 1535.50 nm are out of phase with each other as shown in **Fig. 4(b)**. The reverse of the phase is caused by the difference in the sign of the slope of the U_{dc}. From the measurement using the piezoelectric needle hydrophone with known sensitivity, the acoustic pressure p_{in} was estimated to be 324 kPa. Consequently, the maximum sensitivity S_{BOF} ($=U_{p\text{-}p} / p_{in}$) of the BOF-based ultrasonic hydrophone at 1.56 MHz was calculated to be 5.6 mV/MPa. This value is slightly higher than that of a conventional multilayer hydrophone [4], but for fair comparison, its wide frequency response needs to be clarified.

4. Discussion

In our previous study [6], the sensitivity to the refractive index change of the surrounding media has been clarified. Using this value and the relationship between the sound pressure and the refractive index change, we can calculate the sensitivity to ultrasonic field based on the refractive index modulation of water facing the BOF. However, this sensitivity is almost 10 times smaller than the measured sensitivity 5.6 mV/MPa. Consequently, we can conclude that the stress applied to BOF structure is the major principle of the ultrasonic sensitivity.

5. Conclusion

We demonstrated a trial to apply the BOF-based sensor for mega-hertz ultrasonic-wave detection in water. Ultrasonic waves at 1.56 MHz were experimentally detected with a good SNR. The sensitivity of the sensor at this frequency was 5.6 mV/MPa. This value implied that the stress induced by ultrasonic waves to the BOF has a significant contribution to the ultrasonic sensitivity of BOF.

References

1. J. Staudenraus and W. Eisenmenger: Ultrasonics **31** (1993) 267.
2. D. C. Betz, G. Thursby, B. Culshaw, and W. J. Staszewski: Smart Mater. Struct. **12** (2003) 122.
3. Y. Uno and K. Nakamura: Jpn. J. Appl. Phys. **38** (1999) 3120.
4. W. Weise, V. Wilkens, and C. Koch: IEEE Trans. Ultrason. Ferroelect. Freq. Contr. **49** (2002) 937.
5. K. S. Kim, Y. Mizuno, M. Nakano, S. Onoda, and K. Nakamura: IEEE Photonics Technol. Lett. **23** (2011) 1472.
6. K. S. Kim, Y. Mizuno, and K. Nakamura: Jpn. J. Appl. Phys. **51** (2012) 080202.